

Dynamic characteristic analysis of SCO₂ Brayton cycle under different turbine back pressure modes



Quanbin Zhao, Jiayuan Xu, Min Hou, Daotong Chong*, Jinshi Wang, Weixiong Chen

State Key Laboratory of Multiphase Flow in Power Engineering, Xi'an Jiaotong University, Xi'an 710049, PR China

ARTICLE INFO

Handling editor: Ruzhu Wang

Keywords:

Supercritical carbon dioxide brayton cycle
Dynamic characteristic
Response time
Operation mode

ABSTRACT

Closed supercritical carbon dioxide Brayton cycle has the advantages of high efficiency and high compactness. The response speed of SCO₂ cycle is much faster than that of steam Rankine cycle since the compact system structure and small amounts of heat storage, but the complex mutual effect of multi facilities and closed loop iteration of operation parameters makes the system control difficult. In order to examine the iteration of pressure and temperature in the SCO₂ closed cycle, the dynamic characters of SCO₂ cycle and the related facilities were investigated with different turbine back pressure modes, such as normal operation mode (unconfined back pressure), fixed pressure mode and open loop mode. It has been shown that for different disturbances in the dynamic characteristics of the heat exchanger, the response time of the return heaters is about 4–5 times longer than the response time of the precoolers and heaters. For the dynamic characterization of the SCO₂ cycle in different turbine backpressure modes, the effect of pressure iteration on the SCO₂ system characteristics is less important than that of temperature iteration. In addition, the fixed turbine backpressure operation mode has the advantages of fast response and easy control for the SCO₂ cycle.

1. Introduction

Closed Supercritical carbon dioxide (SCO₂) Brayton cycle is widely researched since the prominent advantages, such as the high compact, high efficiency and high flexibility for different application scenarios, including nuclear power/nuclear power plant, waster heat recovery [1], concentrating solar power plant [2] and coal fired power station [3]. Various system constructions were developed to promote economic [4–6], and kinds of advanced and novel heat exchangers or recuperators were designed to enhance heat transfer under high pressure and temperature [7]. The turbomachinery and its auxiliary accessories were also flourishing [8,9].

As an important part of SCO₂ Brayton cycle, the control system and control strategy also attract wide attentions. A transient analysis code of SCO₂ cycles, named PDC is developed by Moisseytsev and Sienicki [10–13]. Based on the code, the control strategy described by is Dostal is tested with the experimental data from the SNL loop. Carstens [14] develop a simulation code for SCO₂ Brayton cycle named GAS-PASS/CO₂. The effect of special physical property of SCO₂ on the dynamic character of heat exchanger and turbomachinery was researched. And four typical control methods were compared to get high

reliability control strategy for SCO₂ Brayton cycle. Wu et al. [15,16] developed SCTRAN/CO₂ platform for control of supercritical water cooled reactor. The control strategies proposed by Dostal [17] and Moisseytsev [13] were tested for system load up and down, and new control strategies are proposed to prevent nuclear reactor security incidents. Oh et al. [18] researched the control strategy for SCO₂ direct cooling reactors system. The conventional control strategies, such as inventory control strategy, turbine throttling valve control strategy and recuperators bypass control strategies were compared. Wang et al. [19] compared the efficiency and dynamic performance differences of different control strategies in the full load range with considering the safety of the system. They found that inventory control has absolute advantages in terms of efficiency when compared with valve control. However, Berthet [20] found that the precooler bypass control strategy can reduce the effect of environment temperature fluctuation, and improve cycle efficiency for concentration solar heated SCO₂ cycle. Bian et al. [21] put forward five kinds of control strategies with control valves, and found that the turbine bypass valves and HTR bypass valve have a better load regulating ability. Also, the influence of different control valves on the open-loop dynamic performance of the system is investigated. Sun et al. [22] found that under the main steam parameter

* Corresponding author.

E-mail address: dtchong@mail.xjtu.edu.cn (D. Chong).

of 700 °C/35 MP, the connected cycle power generation efficiency of large SCO_2 coal fired power plants is 51.82 %, which is significantly higher than that of available supercritical water-steam Rankine cycle power plants. Li et al. [23] analyzed the safety of UTOP accidents in lead-cooled fast reactors coupled with the SCO_2 cycle and proposed two UTOP accident mitigation schemes based on the SCO_2 cycle.

Furthermore, control strategies were proposed or checked for other conditions, such as Vamshi and Timothy [24] compared different control strategies for low load. Park et al. [25] researched the power swing with valve control method to check SCO_2 system load following capacity. Wang et al. [26] investigated the control strategy for start-up and shutdown of the SCO_2 recompression Brayton cycle. Fuel supply should match the compressor speed control during start-up or shutdown process.

Summarizing previous researches, it is found that although different control strategies for SCO_2 cycle were proposed and applied for different operation processes, control effect were different. On the one side, the SCO_2 systems were different for different researchers, on the other side, the basic dynamic characteristics of SCO_2 cycle is unclear. Therefore, some researchers pay attention to the dynamic characteristics of systems or devices. Carstens [14] found that the fluctuation of temperature and pressure at precooler outlet and high temperature heater have great effect on system operation efficiency and the system response speed. Singh et al. [27] investigated the disturbance of environment temperature and solar energy input on concentrating solar power plant with SCO_2 cycle, the effect of environment temperature on precooler can affect system performance a lot. Olumayegun and Wang [28] built a dynamic model of SCO_2 cycle for industrial waste gas utilization. The fluctuation of waste gas mass flow rate and temperature were found have great effect on dynamic character of SCO_2 cycle. Hu et al. [29] calculated the dynamic response characteristic of the recuperator when system power ratio gradually decreased from 100 % to 50 %. There was an intersection between the hot/cold fluid temperature curves under different generation loads. Deng et al. [30] developed a dynamic model of the SCO_2 recompression Brayton cycle and examined the effects of high-temperature and low-temperature recuperator on the dynamic characteristics of the cycle.

The dynamic character is very important for the system control strategy development and safety operation of SCO_2 Brayton cycle. The

complex mutual effect of multi facilities and closed loop iteration of operation parameters makes the system control difficult, more important is that the iteration of pressure and temperature in closed SCO_2 cycle were still not clear. In this paper, the dynamic characters of SCO_2 cycle and the related facilities were investigated with different turbine back pressure modes, such as normal operation mode (unconfined back pressure), fixed pressure mode and open loop mode. It aims to reveal the interaction characteristic and restrictive relation of SCO_2 cycle, which is meaningful to the development of system control strategy and control parameters.

2. SCO_2 cycle system and the simulation model

2.1. SCO_2 cycle system

In this paper, an optimized recompression SCO_2 cycle configuration is designed for the Fluoride-salt-cooled High-temperature Reactor(FHR), as shown in Fig. 1. FLiBe is used as the coolant for the FHR, and FLiNaK is used in the intermediate loop for heat exchange with the SCO_2 Brayton cycle system. These two types of molten salt have high boiling point temperature and low flow viscosity at atmospheric pressure, which can fit the FHR operation requirement. Considering the long-term stable operating temperature of metallic materials, the reactor outlet temperature is set as 700 °C. Moreover, considering molten salt liquidity and lower thermal stresses of Hastelloy, the inlet temperature of the reactor is set as 600 °C [31,32]. For the heat transfer in FHR, the heat exchanger end difference between FLiBe and FLiNaK is set as 20 °C, and it is 30 °C between FLiNaK and SCO_2 . As a result, the temperature of heat source can reach to 700 °C, and the maximum operation temperature for SCO_2 Brayton cycle system is 650 °C. Other key parameters of SCO_2 cycle are listed in Table 1. However, this paper mainly focuses on the dynamic character of SCO_2 cycle, the dynamic character of fluoride reactor and the interaction effect between SCO_2 cycle and fluoride reactor is not considered at present research.

2.2. Simulation model for SCO_2 cycle

1) Compressor model

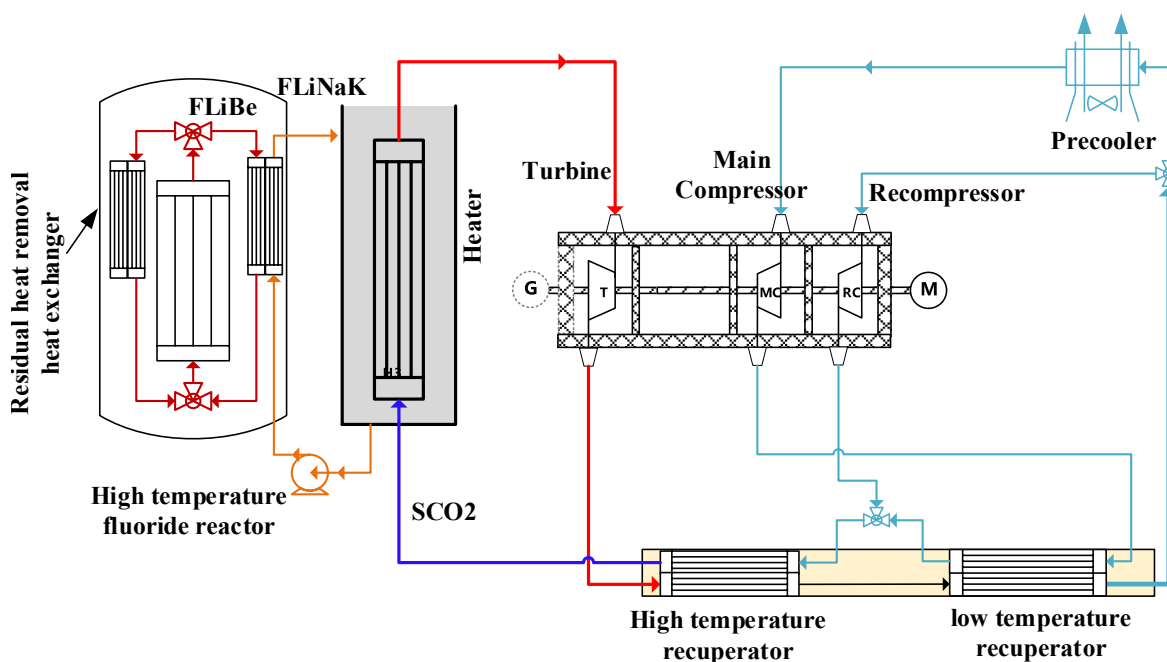


Fig. 1. The designed configuration of SCO_2 cycle for fluoride reactor.

Table 1The designed key parameters of SCO₂ cycle for fluoride reactor.

Parameters	Value	Parameters	value
Heat power (MWt)	15	Pressure at main compressor outlet, $P_{C\text{-out}}$ (MPa)	25.03
Temperature at turbine inlet, $T_{T\text{-in}}$ (°C)	650.0	Pressure at Re-compressor inlet, $P_{RC\text{-in}}$ (MPa)	8.58
Temperature at turbine outlet, $T_{T\text{-out}}$ (°C)	514.4	Pressure at Re-compressor outlet, $P_{RC\text{-out}}$ (MPa)	25.02
Temperature at main compressor inlet, $T_{C\text{-in}}$ (°C)	35.0	Pressure at turbine inlet, $P_{T\text{-in}}$ (MPa)	25.0
Temperature at main compressor outlet, $T_{C\text{-out}}$ (°C)	69.0	Pressure at turbine outlet, $P_{T\text{-out}}$ (MPa)	8.63
Water temperature at precooler inlet, $T_{water\text{-in}}$ (°C)	20.0	SCO ₂ mass flow rate, m_{SCO_2} (kg/s)	64.58
Temperature at Re-compressor inlet, $T_{RC\text{-in}}$ (°C)	206.9	efficiency of main compressor	0.850
Temperature at Re-compressor outlet, $T_{RC\text{-out}}$ (°C)	182.9	efficiency of Re-compressor	0.850
Split ratio	0.32	efficiency of turbine	0.897
Pressure at main compressor inlet, $P_{C\text{-in}}$ (MPa)	8.57	efficiency of SCO ₂ cycle	0.486

Considering the cycle output power is in the level of megawatt, a radial flow main compressor and re-compressor is selected. And the model and correlations of compressor used by Dyreby [33] can be as a reference, and the compressor similarity principle [34] is used to adjust the compressor performance curve to match SCO₂ cycle in this paper. The adjusted performance curves for main compressor and re-compressor are shown in Figs. 2 and 3.

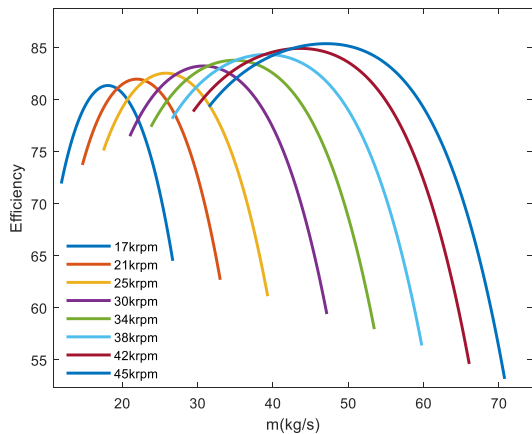
2) Turbine model

The Stodola's ellipse method is applied here for the off-design calculation of the SCO₂ turbine with the assumptions of sliding pressure operation [35]. Applying the Stodola's ellipse method, the off-design mass flow coefficient is calculated as follows:

$$\frac{\varphi_{od}}{\varphi_d} = \frac{\sqrt{1 - (p_{out,od}/p_{in,od})^2}}{\sqrt{1 - (p_{out,d}/p_{in,d})^2}}$$

where φ_d and φ_{od} are the mass flow coefficient under design and off-design conditions. φ is then defined as follows:

$$\varphi = m_{in} \frac{\sqrt{T_{in}}}{p_{in}}$$



(a) Efficiency of main Compressor

The isentropic efficiency of the turbine under off-design conditions can be obtained as follows:

$$\eta_T = \eta_{T,d} \sin \left[0.5\pi \left(\frac{m_{in}\rho_{in}}{m_{in,d}\rho_{in,d}} \right)^{0.1} \right]$$

where $\rho_{in,d}$ and $\rho_{in,d}$ are the density of CO₂ under design and off-design conditions.

3) model of heat exchanger

In SCO₂ cycle, the heat exchangers play key role for system operation with high efficiency, also their volumes occupy the main position in the system, which lead to the long response time in transient operation process. According to previous research, the PCHE can meet the operation requirement for the precooler cooled with water, recuperator and heater heated by fluoride. Thus, the counter flow with straight channels type of PCHEs are used in SCO₂ cycle and the simplified one-dimensional models are built. Heat exchangers are divided into hot side working medium, cold side working medium and metal wall. And the heat exchangers are divided into many nodes along flow directions. In each node, the cold fluid control body, hot fluid control body and metal wall are included, as shown in Fig. 4. Furthermore, a few of assumptions are listed as follows.

- (1) The parameters and heat transfer in each node is dealt with lumped parameter method;
- (2) The arithmetic mean temperature difference is used to calculate heat transfer character in each node;
- (3) The heat conduction along the flow direction for metal wall is neglected.

In each node of heat exchanger, the mass conversation equation and energy conversation equation were used.

Mass conservation equation (taking node 2 as example):

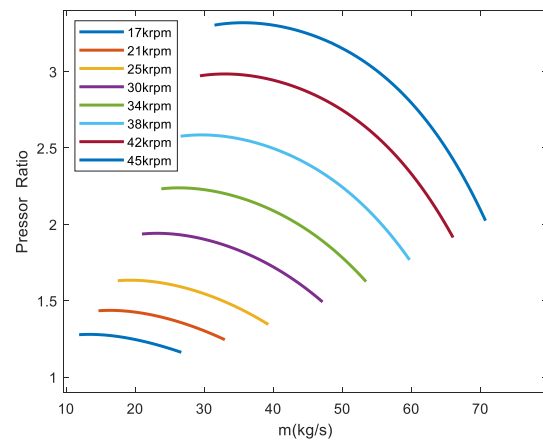
$$V \frac{d\rho}{d\tau} = m_{in} - m_{out}$$

Energy conservation equation for hot side:

$$V \frac{d(\rho h)}{d\tau} = m_{in}h_{in} - m_{out}h_{out} - Q_{hot}$$

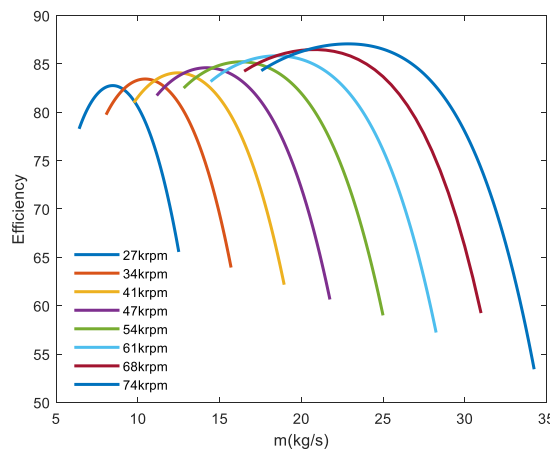
Energy conservation equation for cold side:

$$V \frac{d(\rho h)}{d\tau} = m_{in}h_{in} - m_{out}h_{out} + Q_{cold}$$

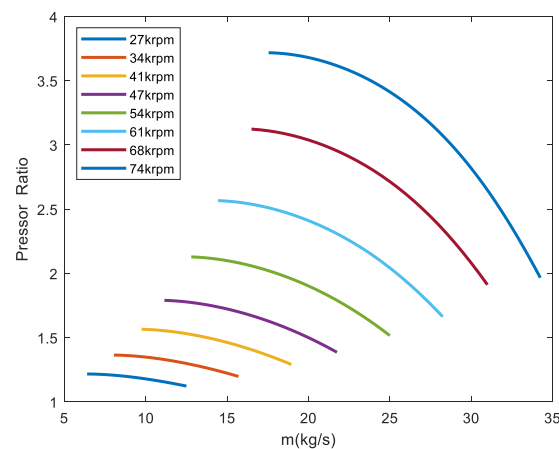


(b) Pressure ratio of main Compressor

Fig. 2. Efficiency and pressure ratio of main compressor.



(a) Efficiency of Re-Compressor



(b) Pressor ratio of Re-Compressor

Fig. 3. Efficiency and pressure ratio of Re-compressor.

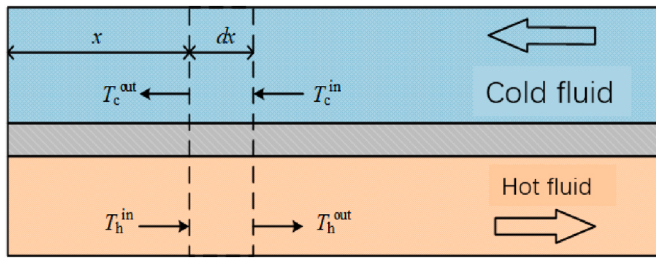


Fig. 4. Simulation model of heat exchanger.

Energy conservation equation for mental wall:

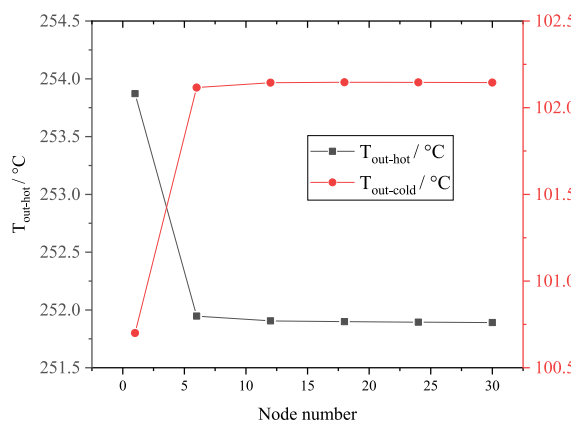
$$M_w C_w \frac{dT_{w-hot}}{dt} = Q_{hot} - Q_w$$

And the storage heat in liquid metal can be obtained with equation

$$M_w C_w \frac{dT_{w-cold}}{dt} = Q_w - Q_{cold}$$

The heat transfer coefficient for water in precooler is calculated with Dittue-Boelter correlation

$$Nu = 0.023 Re^{0.8} Pr^{0.3}$$



(a) node number for heat exchanges

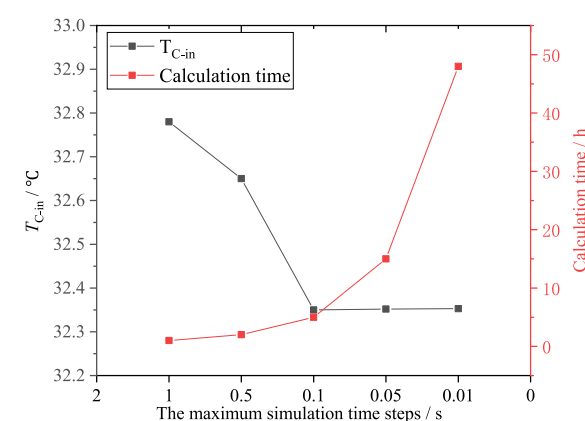


Fig. 5. Model verification.

(b) Simulation time step

experimental results reported by Ma et al. [36], it is found that the dynamic simulation results of both inlet and outlet parameters can match experimental data well, as shown in Fig. 6. The maximum predicted error is less than 2.0 %, which indicates the simulation model can calculate the dynamic character of SCO_2 cycle accurately.

3. Results and discussion

3.1. Dynamic character of key heat exchanger in SCO_2 cycle

The SCO_2 flow velocity in compressor and turbine is sonic or transonic, the response time of these facilities is approach zero seconds when compared to the response time of heat exchanger. The dynamic performance of turbomachinery is approximate to their own property, which have been shown in Section 2. Thus, only the dynamic character of heat exchanger will be investigated in this part.

Since the dynamic character of heat exchanger is closely related to the heat transfer power and the size of heat exchanger, these parameters are shown in Fig. 7, which were calculated based on the designed parameters shown in Table 1. The heat power of recuperators obviously larger than heater and precooler, and the volumes of recuperators are also larger. It should be that the response time of recuperators should be longer, especially for high temperature recuperator (HTR). The precooler and heater volumes are much smaller than the recuperator, mainly because the total heat transfer coefficients of the precooler and heater are relatively large, and the total heat transfer coefficients of the pre-cooler, the heater and the return heaters for the design conditions are given in Table 2.

Then dynamic characteristics of heat exchangers under different parameters disturbance are investigated, such as the inlet temperatures, inlet pressures and mass flow rates. The pressure response speed is much fast than temperature, and the change amplitude is very small for single heat exchanger, thus the pressure response character is not discussed in this paper. Fig. 8 shows the dynamic characteristics of outlet temperature at hot side under different disturbance of inlet temperature at cold side. The outlet temperatures of all heat exchangers show positively correlation with inlet temperature at cold side. The difference is that the temperature response curve for precooler is asymmetrical when temperature disturbance amplitude is opposite. This is caused by the special SCO_2 feature near critical point. When the inlet temperature of precooler at cold side decrease, the SCO_2 temperature would decrease, which would go closer to the SCO_2 critical temperature, where the specific heat and density would increase obviously.

Furthermore, the response time and change amplitude for different

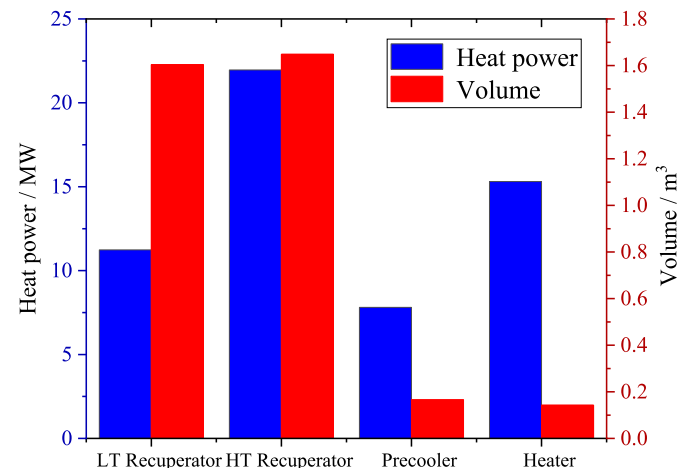


Fig. 7. Heater volume and heat power for each heat exchanger in SCO_2 cycle.

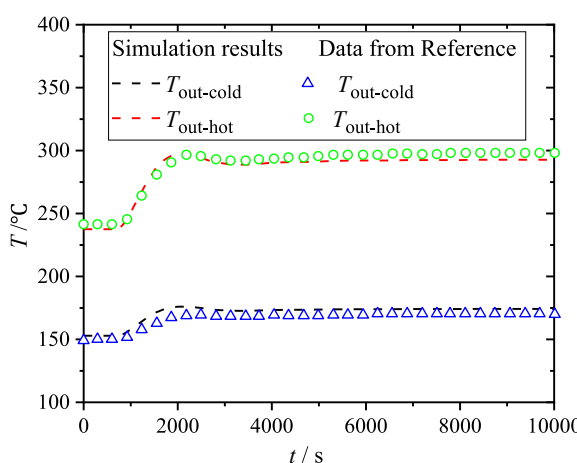
Table 2

Total heat transfer coefficient for different heat exchangers at design conditions.

Heat exchanger	Total heat transfer coefficient/W/($\text{m}^2 \cdot \text{K}$)	Heat exchanger	Total heat transfer coefficient/W/($\text{m}^2 \cdot \text{K}$)
HTR	633.86	LTR	999.41
Heat	1865.73	PC	1742.27

heat exchangers are summarized., as shown in Fig. 9. The response time of recuperator are much longer than that of precooler and heater, and heater's response time is shortest among them. With rise of temperature change, the response time increases gradually. The response time of recuperator is about 35–40 s when temperature disturbance amplitude is about 5 °C, but it is about 10–15 s for precooler and 10 s for heater. The outlet temperature at hot side under different disturbance are also different. The outlet temperature of high temperature recuperator seems much more sensitive to the inlet temperature disturbance, but outlet temperature of heater is least sensitive.

The dynamic response character of heat exchanger under heat transfer fluid flow rate disturbance is similar to that temperature disturbance, as shown in Fig. 10. The response time of high temperature recuperator and low temperature recuperator is longer than that of precooler and heater. With increasing of mass flow rate disturbance amplitude, the tendency of response time shows increasing at first and



(a) Recuperator

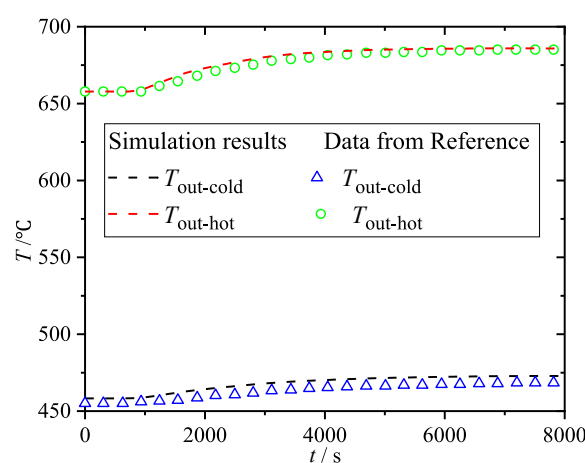


Fig. 6. Model verification for heat exchangers.

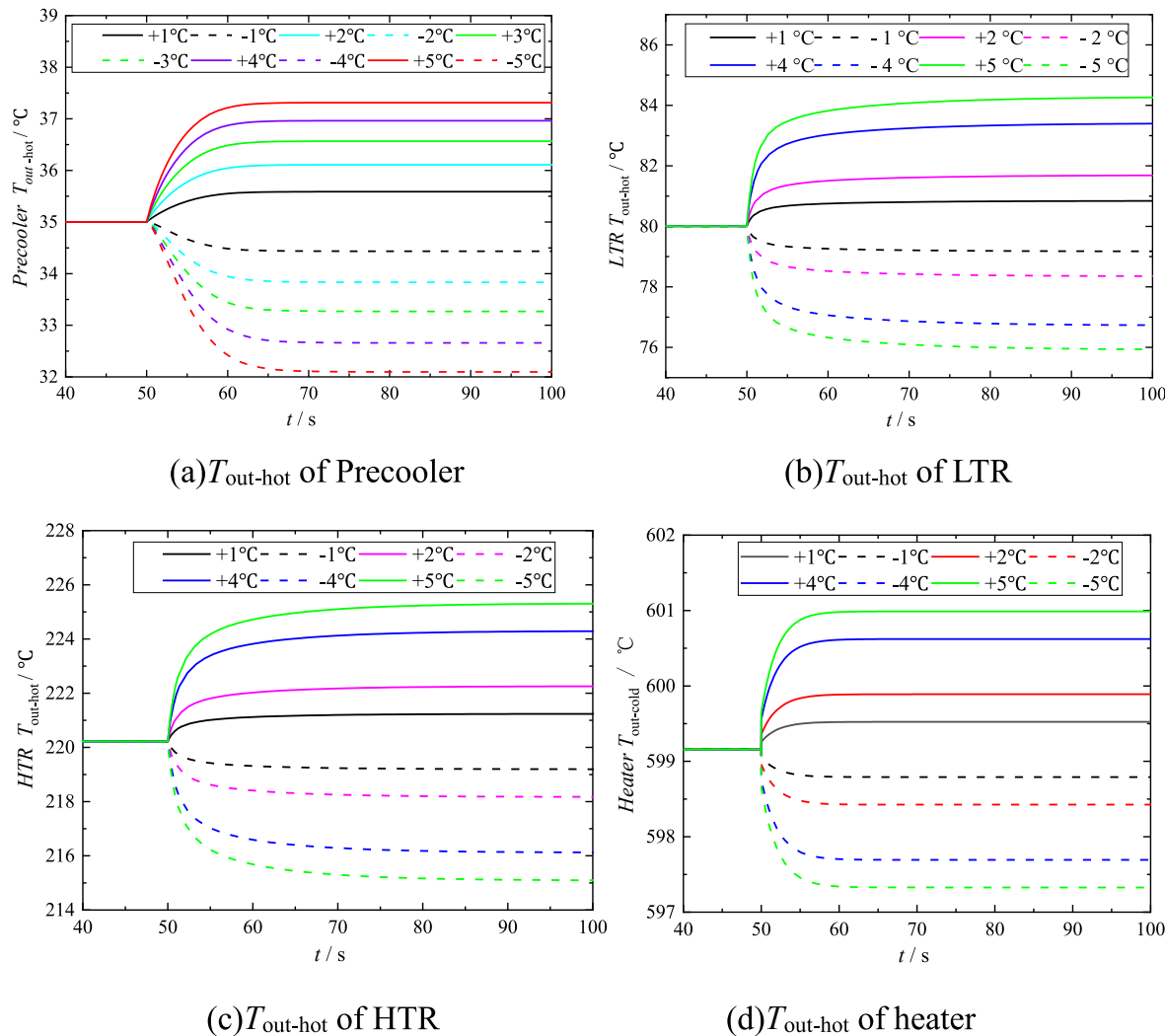


Fig. 8. Dynamic response characteristics of heat exchangers under temperature disturbance.

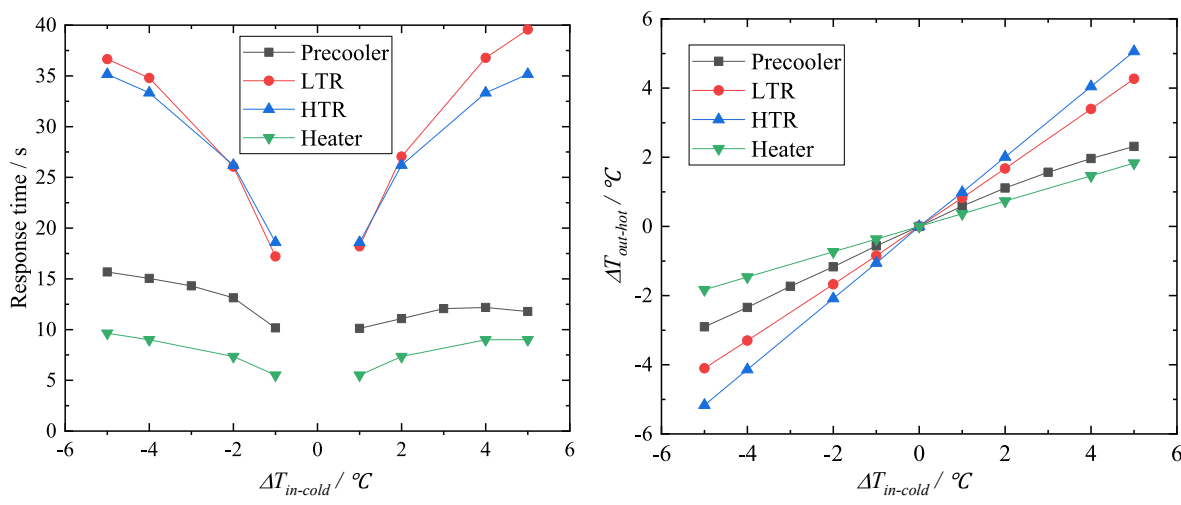
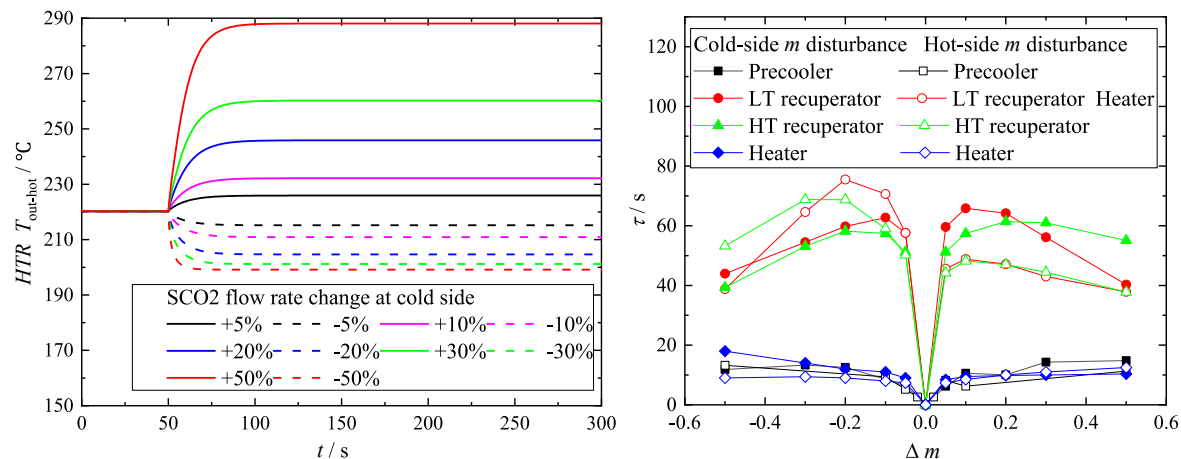
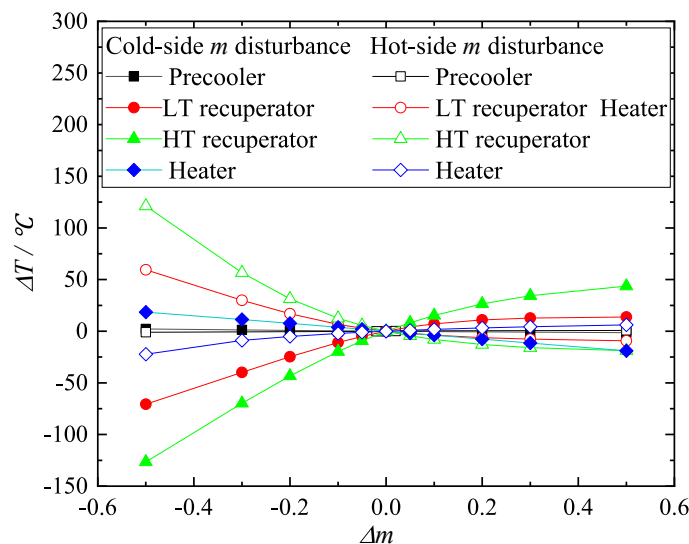


Fig. 9. Dynamic response characteristics of heat exchangers under temperature disturbance.

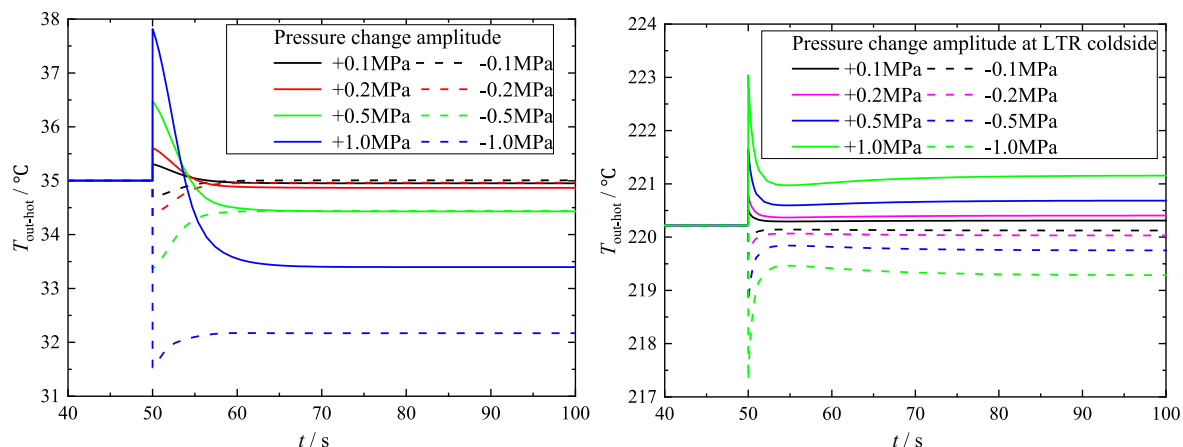


(a) Dynamic characteristics of HTR (b) Response time for different heat exchangers



(c) Temperature change amplitudes at heat exchanger outlet

Fig. 10. Dynamic response characteristics of heat exchangers under heat transfer fluid flow rate disturbance.



(a) Pressure disturbance at precooler hot side (b) Pressure disturbance at LTR hot side

Fig. 11. Dynamic character of heat exchangers to operation pressures disturbance.

then decreasing. The maximum response time present at $\Delta m = \pm 20\%m$, approximately. Under present test conditions, the response time of recuperator is about 40–80 s, and it is 5–20 s for other heat exchangers.

The outlet temperature change amplitude is shown in Fig. 10(c) under different heat transfer fluid mass flow rates. It is found that the temperature change amplitudes for recuperators are larger than others. The maximum temperature change amplitude of high temperature recuperator can reach to 125 °C when fluid mass flow rates decrease to the half of designed mass flow rate. However, the maximum temperature change amplitude for precooler is lower than 2 °C, which attributes to the large specific heat near the SCO_2 critical point. The temperature change amplitudes under fluid mass flow rate decreasing conditions are larger than that mass flow rate increasing conditions obviously.

The disturbance of operation pressures on outlet temperature and pressure of heat exchanger are investigated, as shown in Fig. 11. Fig. 11(a) shows the SCO_2 temperature response characteristic of precooler to SCO_2 pressure disturbance. The temperatures at precooler outlet show a step change and then decrease gradually, which is owed to the pressure disturbance transfer speed in heat exchanger much faster than temperature disturbance transfer speed. However, due to the heat storage in metal wall, the SCO_2 temperature will changes gradually until to heat and mass transfer reached to balance state in heat exchanger. The dynamic characters of recuperator and heater are similar to the precooler, as shown in Fig. 11(b). However, when the SCO_2 pressure change amplitude is very large in precooler, the SCO_2 temperature at precooler outlet will decrease, which is quite different from other heat exchangers. The special dynamic character of pressure disturbance will lead the dynamic character of SCO_2 cycle system complex and make the system control difficult.

Fig. 12(a) shows the response time of outlet temperature of heat exchangers under different pressure disturbance. The maximum response time of recuperators is about 50 s and it is less than 15 s for precooler and heater. Furthermore, the effect of pressure step disturbance on outlet temperature is shown in Fig. 12(b). The change amplitudes of outlet temperature are no more than ± 3 °C under present test conditions. And for precooler, the SCO_2 pressure disturbance will always lead SCO_2 outlet temperature decrease.

3.2. Dynamic character of SCO_2 cycle under cold end parameter disturbance

Considering the SCO_2 Brayton cycle is a complete closed loop, system parameters may iterate many times as disturbance occurs, and the

dynamic character would be different from the dynamic feature of single device or the superposition of single devices. Therefore, the dynamic characteristics of SCO_2 cycle are investigated in this paper. According to the SCO_2 cycle character, all the operation parameters, such as SCO_2 temperature, pressure and mass flow rate have great effect on system performance, and they are closely associated with each other, which make the analysis for system dynamic character difficult. For the convenience of analyzing, two additional operation modes are investigated and compared. One operation mode is that the pressure at turbine outlet is fixed with a pressurizer (named as Fixed back pressure mode). Then the pressure iteration in the closed loop would be break, which is also used by previous researchers. As a comparison, the operation mode with an opened SCO_2 cycle is investigated. The cutting open point is at the position where parameter disturbance occurs (named Open cycle mode).

Fig. 13 shows the dynamic response characters of system key parameters under cooled water flow rate step disturbance at precooler. Obviously difference existed between the fixed back pressure mode and normal operation mode. The change amplitude of system parameters, including temperatures, pressures and SCO_2 mass flow rates under normal operation mode is much larger than that under fixed back pressure mode, except SCO_2 temperature at precooler outlet. This means the normal operation mode system seems more sensitive to the water flow rate.

Among the three different operation modes, both the change amplitudes of SCO_2 temperature and pressure at precooler outlet with normal operation mode is smallest, and a temperature turning point present when water flow rate decreases by 30 %, as shown in Fig. 14, which is different from those with fixed back pressure mode and open cycle mode. Then tendency of SCO_2 temperature and pressure at precooler outlet with fixed back pressure mode and open cycle mode are similar, and the change amplitude of SCO_2 pressure at precooler outlet with open cycle mode is largest, which indicates that temperature iteration also has great effect on pressure of SCO_2 cycle. The small change amplitude of temperature at precooler outlet will lead to small pressure changes, which can be used for the cold end temperature and pressure control.

The effect of operation model on system dynamic character is analyzed with Fig. 15. The dynamic operation character of key parameters under fixed backpressure operation model, normal operation mode, and open cycle mode are compared under conditions of water flow rate change amplitude of $\pm 50\%$. Overall, all parameters have a fast response to the water flow rate disturbance within 50 s. That is partly due to the response time of precooler is about 50 s. On the other hands, it

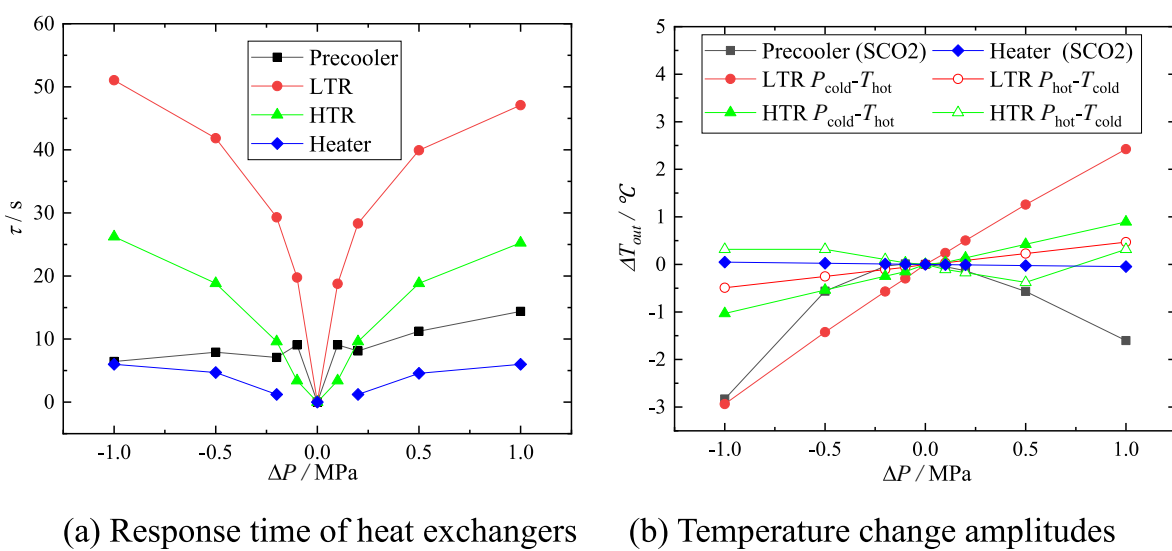


Fig. 12. Parameter response of heat exchangers to pressure disturbance.

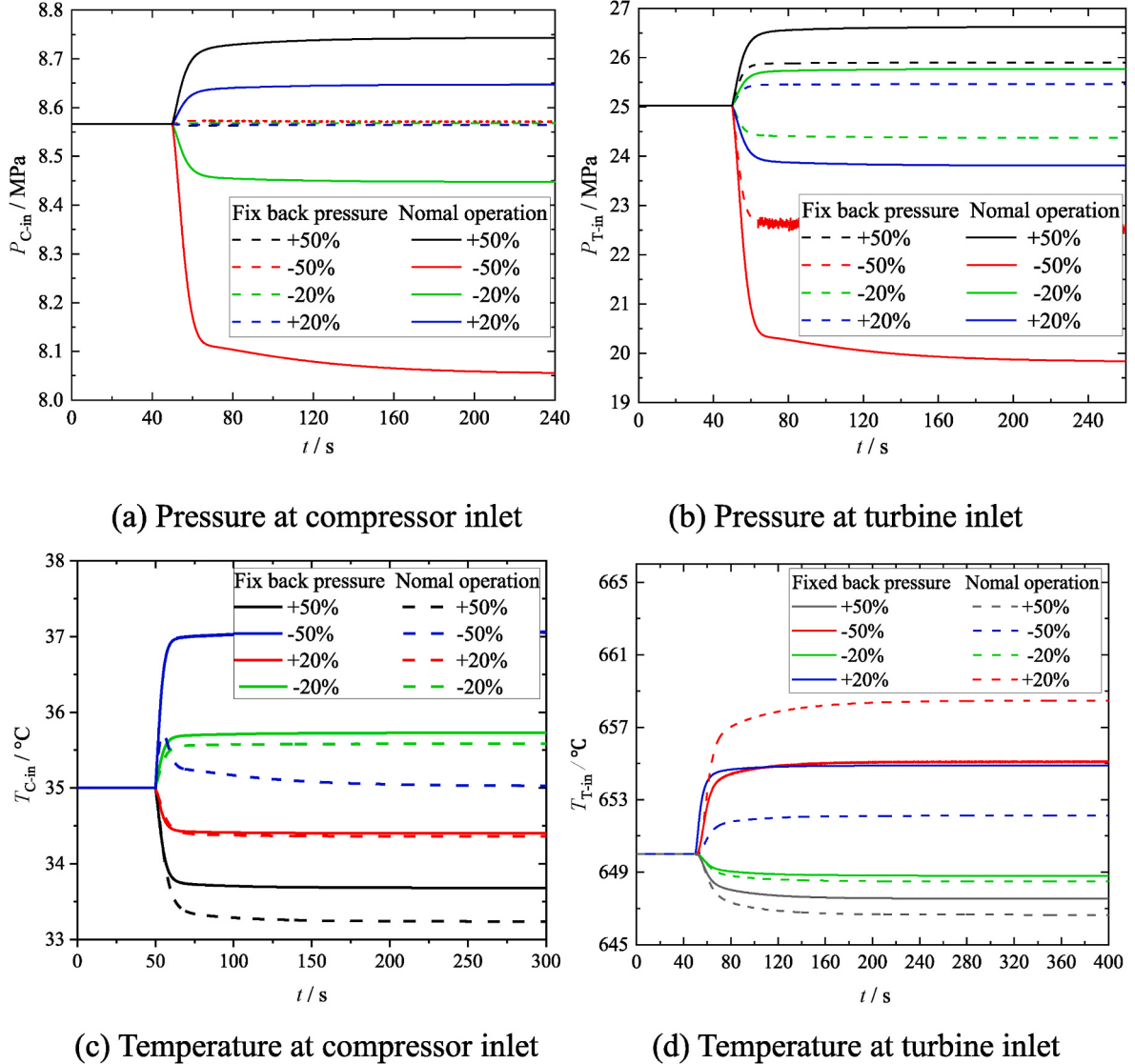


Fig. 13. Dynamic response characteristics of parameters under cooled water flow rate step disturbance at precooler.

is attributed to the fast propagation speed of pressure in the system. Then the parameter response line become gently, which is attributed to the slowly transfer characteristic of temperature at HTR and LTR, and the iteration feature of temperature. Moreover, under the open cycle mode, the temperature at compressor inlet is great affected by water flow rate and the then compressor outlet pressure change a lot within 50 s. But in a later period of time, the parameters tend to stabilize rapidly since the effect of temperature change amplitude become small in the heat exchangers downstream. But under the fixed backpressure operation model, normal operation modes, the dynamic responses time of SCO_2 cycle is much longer than that with open cycle mode. Although the pressure iteration effect is eliminated for fixed back pressure mode, the temperature and SCO_2 flow rate iteration still have great effect on system dynamic characteristic, and the response characteristics with normal operation mode and fixed back pressure mode shows similar response character.

Due to the complex effect of temperature and pressure on system response characteristics and the complex SCO_2 physical properties, the temperature change amplitudes of SCO_2 cycle at different positions were summarized, as shown in Fig. 16. The temperature change amplitudes of high temperature recuperator are the largest, and temperature change amplitudes of low temperature recuperators take the second

place. Therefore, the response time of recuperators are much longer than others (as shown in Fig. 15), which also leads to the system response time is long.

The dynamic response time for different operation models is compared, as show in Fig. 17. The response time of normal operation mode is longer than other two modes. The system response time is about 220–370 s for normal operation mode and 200–250 s for fixed back pressure mode. They are much longer than response time with open cycle mode. And the response time under water flow rate reduction scenarios is much longer than that under water flow rate rising scenarios. It may be attributed to the large specific heat capacity of SCO_2 near the critical point and small change amplitude of compressor inlet temperature. The response time difference for different operation modes under the same water flow rate step amplitude may owe to the iteration of SCO_2 temperature and pressure, and the system parameter disturbance can be strength by the compressor greatly.

Furthermore, the SCO_2 cycle efficiency, compressor efficiency and turbine efficiency are summarized in Fig. 18. Under normal operation mode, the efficiencies change slightly for different water flow rates. And the efficiencies under the normal operation mode and fixed back pressure mode have little difference when water flow rate ranges from 80 % m_{design} to 150 % m_{design} . However, when water flow rate decreased to 70

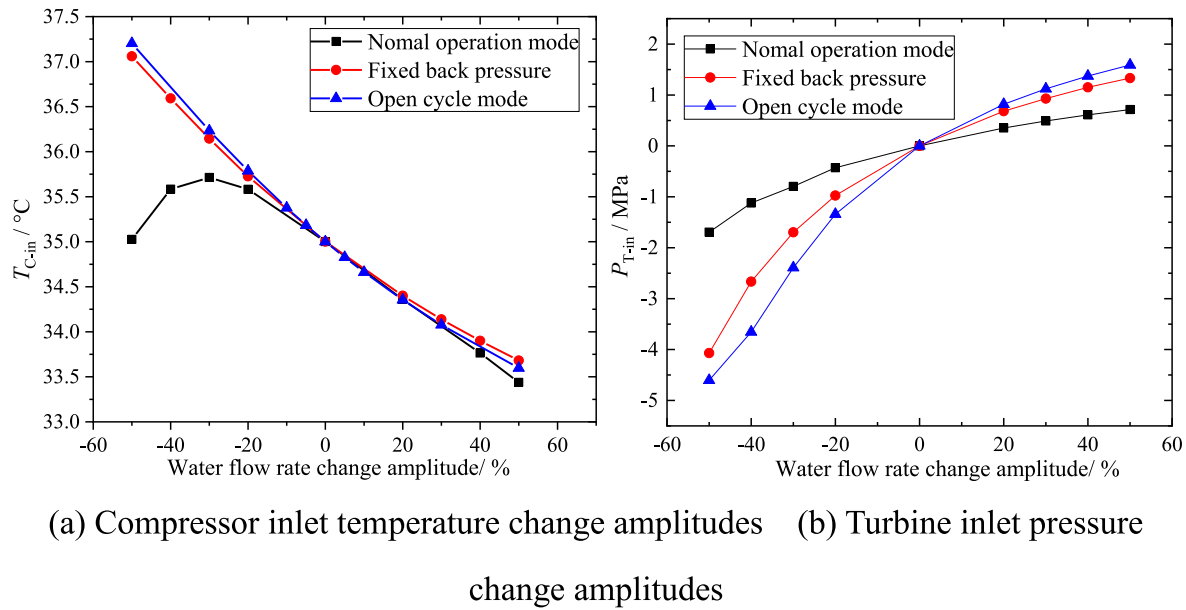
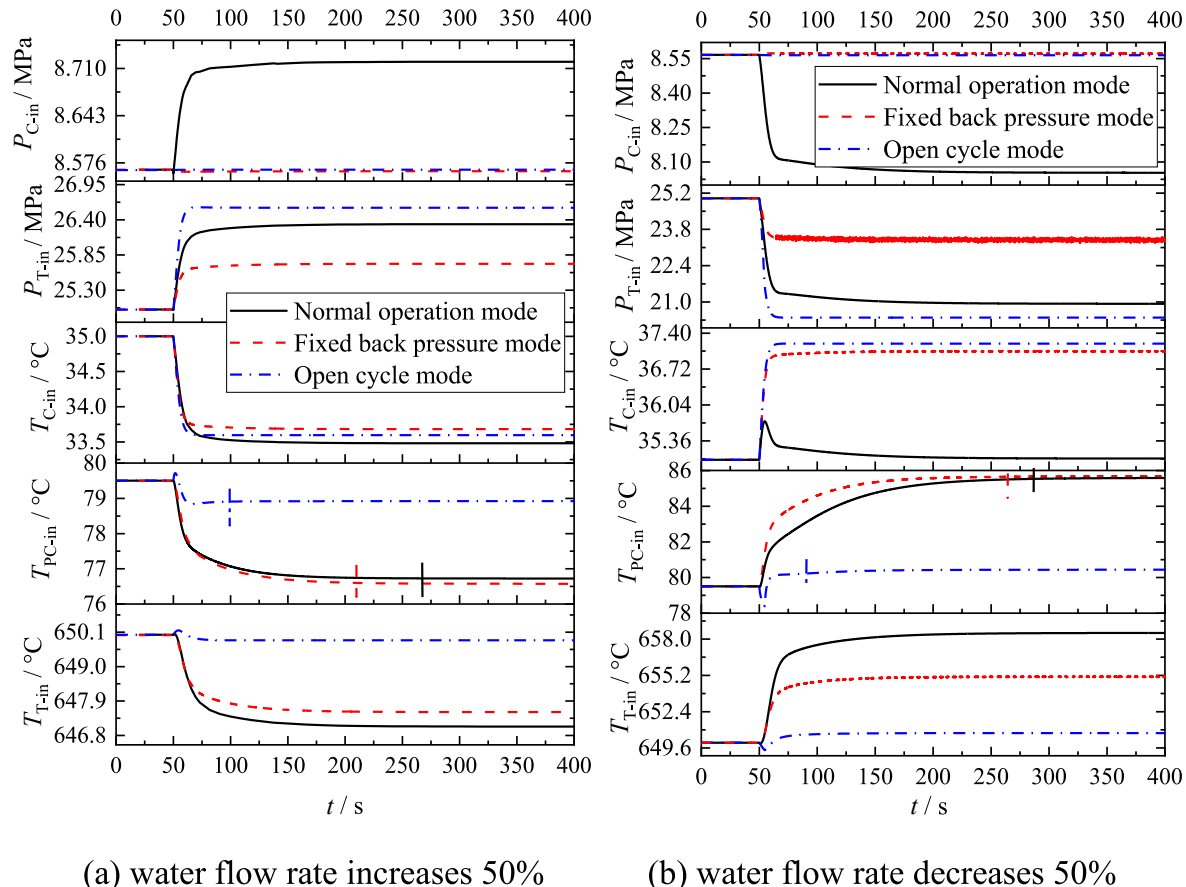


Fig. 14. Dynamic response characteristics of parameters under cooled water flow rate step disturbance at precooler.



(a) water flow rate increases 50%

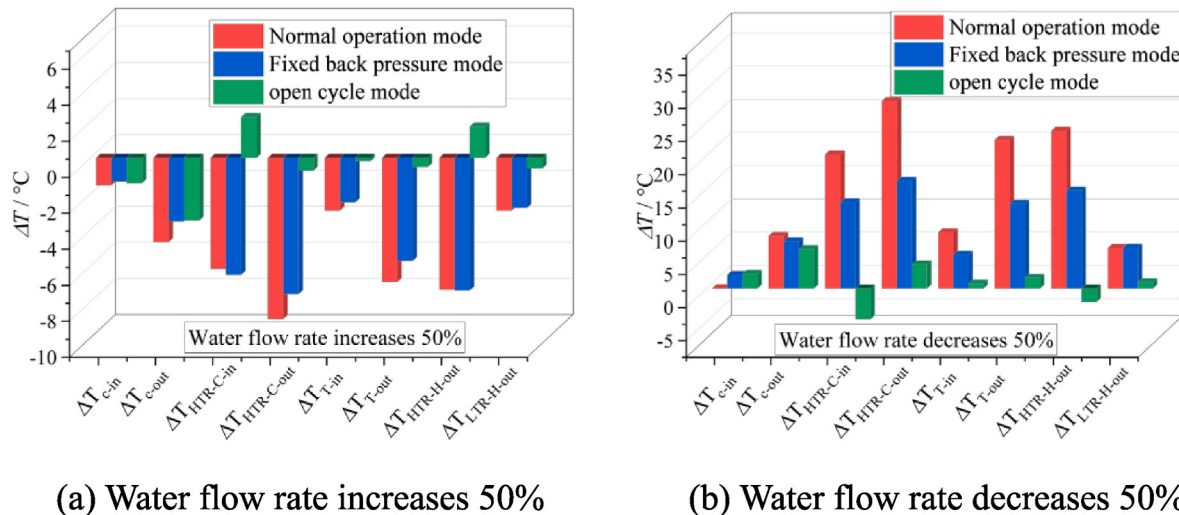
(b) water flow rate decreases 50%

Fig. 15. Dynamic response lines for key parameters under water flow rate disturbance with different operation mode.

$\%m_{\text{design}}$, the SCO_2 cycle efficiency, compressor efficiency and turbine efficiency would decrease rapidly under normal operation mode. The dynamic character of SCO_2 cycle system under water temperature disturbance is similar with that under water flow rate disturbance, which are not discussed in this paper.

3.3. Dynamic character of SCO_2 cycle under heat source parameter disturbance

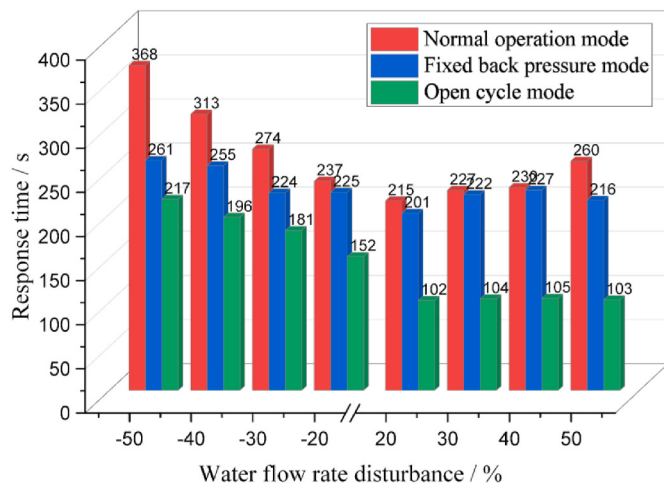
Fig. 19 shows the dynamic character of SCO_2 cycle under the disturbance of heat fluorine flow rate for different operation modes. The temperatures at compressor inlet are similar under different operation



(a) Water flow rate increases 50%

(b) Water flow rate decreases 50%

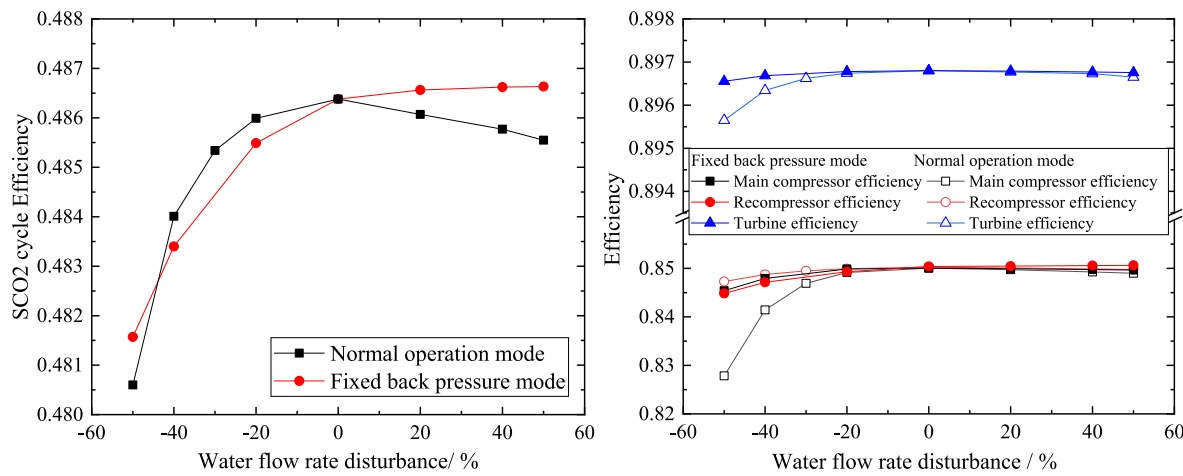
Fig. 16. Temperature change amplitudes for key parameters under water flow rate disturbance with different operation mode.

Fig. 17. Response time of SCO₂ cycle under water flow rate disturbance with different operation mode.

modes. The maximum pressure change amplitude of compressor inlet pressures are also less than 0.01 MPa, which has less effect on compressor efficiency and pressure ratio, as shown in Fig. 19(a) and (b). Fig. 19(c) and (d) show the response characteristics of turbine inlet pressure and temperature under fluorine flow rate disturbance. The change amplitudes of turbine inlet temperature under the normal operation mode and fixed back pressure are similar and small pressure difference between the two operation modes.

Fig. 20 summarized the turbine inlet temperature and pressure when SCO₂ cycle return to steady state after the disturbance. Also, the results under normal operation mode, fixed back pressure mode and open cycle mode were compared. The change amplitudes of turbine inlet temperature and pressure for SCO₂ cycle are larger than that with open cycle mode, since the main compressor in SCO₂ cycle will enlarge the effect of disturbance. For the same reason, the change amplitude of turbine inlet pressure under normal operation mode is larger than that under fixed back pressure mode.

Fig. 21 shows the comparation of system parameters response characteristics under heat fluorine flow rate disturbance. When heat fluorine flow rate changes, the turbine inlet temperature responses quickly within 25 s. So do the turbine inlet pressure and compressor inlet pressure. Similar to that with water flow rate disturbance, the response

(a) SCO₂ cycle efficiency

(b)Compressor and turbine efficiency

Fig. 18. Efficiency of SCO₂ cycle and turbomachines under water flow rate disturbance with different operation mode.

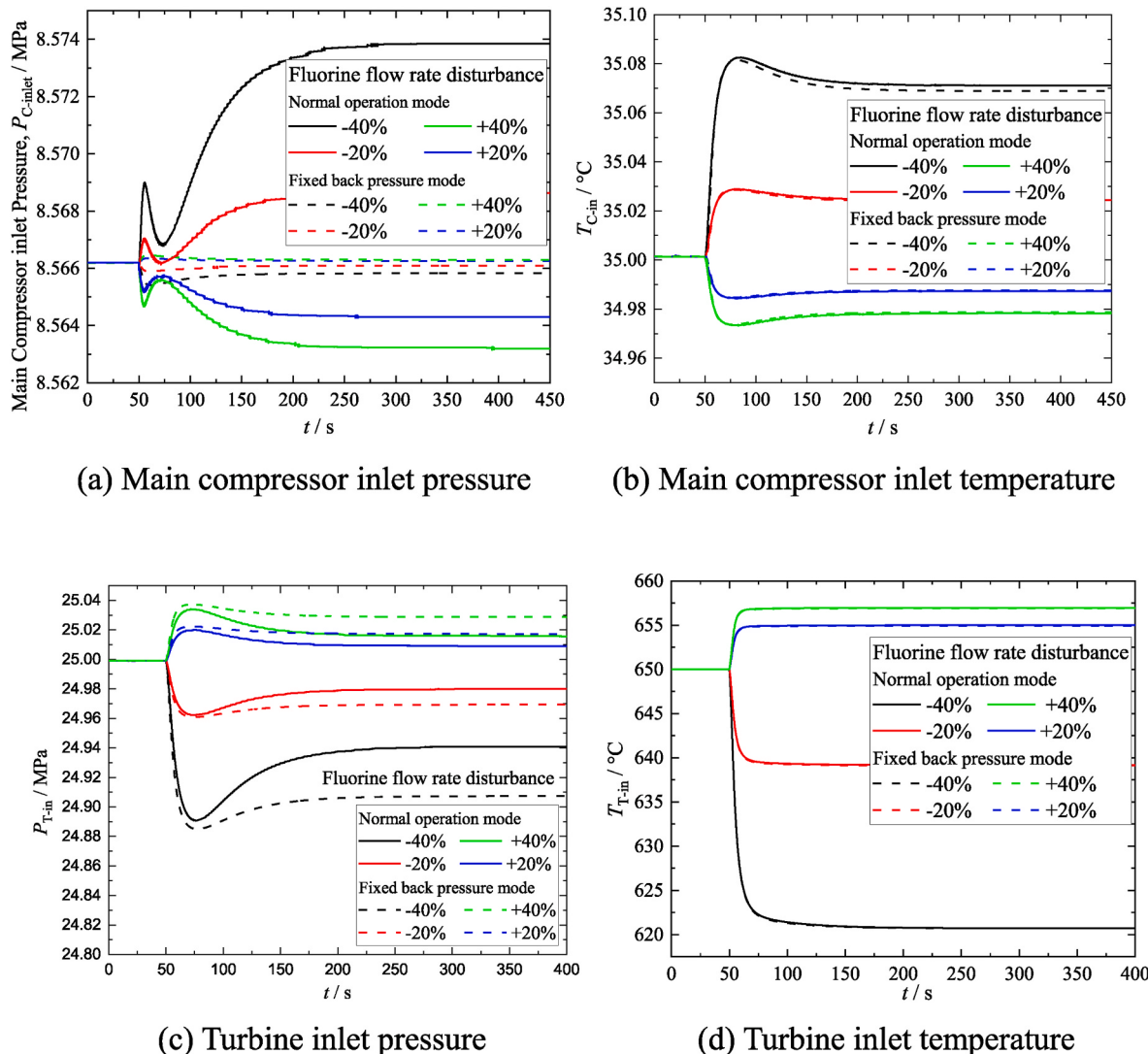


Fig. 19. Dynamic response characteristics of parameters under fluorine flow rate step disturbance at heater.

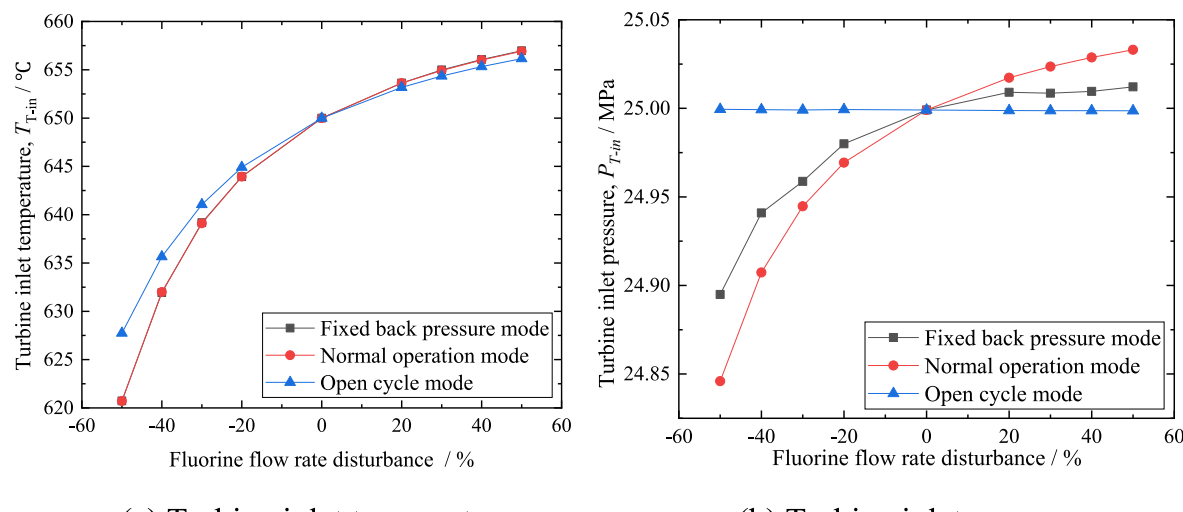


Fig. 20. Dynamic response characteristics of parameters under cooled water flow rate step disturbance at precooler.

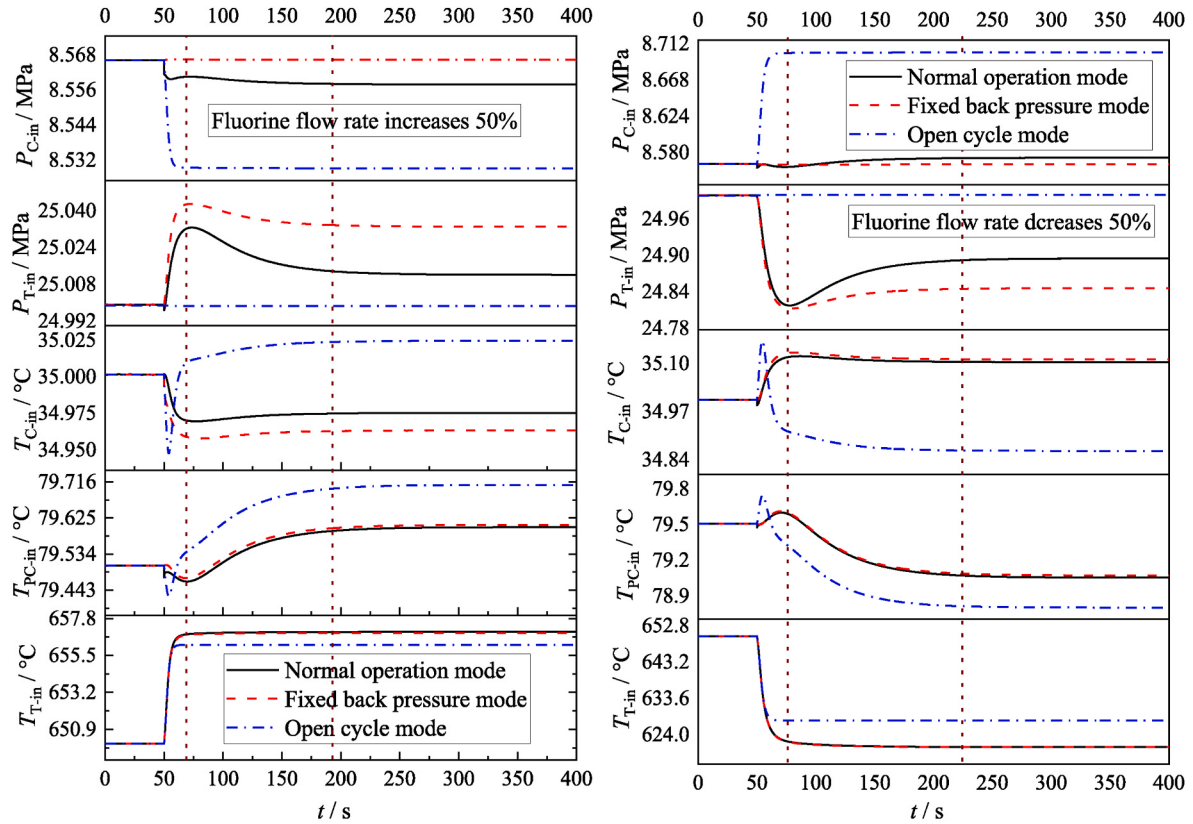


Fig. 21. Dynamic response lines for key parameters under fluorine flow rate disturbance with different operation mode.

time of the high temperature recuperator and low temperature recuperator is longer than others, which leads to the response time of SCO_2 cycle reaches to 250 s, approximately. The slowly temperature tends at recuperators make the pressure and temperature at compressor inlet changes gradually. Then with the joint influence of compressor inlet pressure and temperature, the compressor pressure ratio changes, and turbine inlet pressure changes until the compressor inlet temperature stabilizes.

When the temperatures at different equipment are compared under the same heat fluorine flow rate disturbance, such as $\pm 50\%$ shown in

Fig. 22, the temperatures at turbine inlet and outlet change obvious since they are affected by heat fluorine flow rate directly. The temperatures at recuperators also change a lot, which have great effect on SCO_2 cycle response time. The temperature at compressor inlet changes little, therefore the compressor feature is almost unaffected.

Fig. 23(a) shown the comparison of response time under different modes. The response time with fixed pressure mode is approximately equal to that under open cycle mode, which indicates that the temperature change amplitude become small at compressor inlet and the iteration of temperature can be neglected. The response time with normal

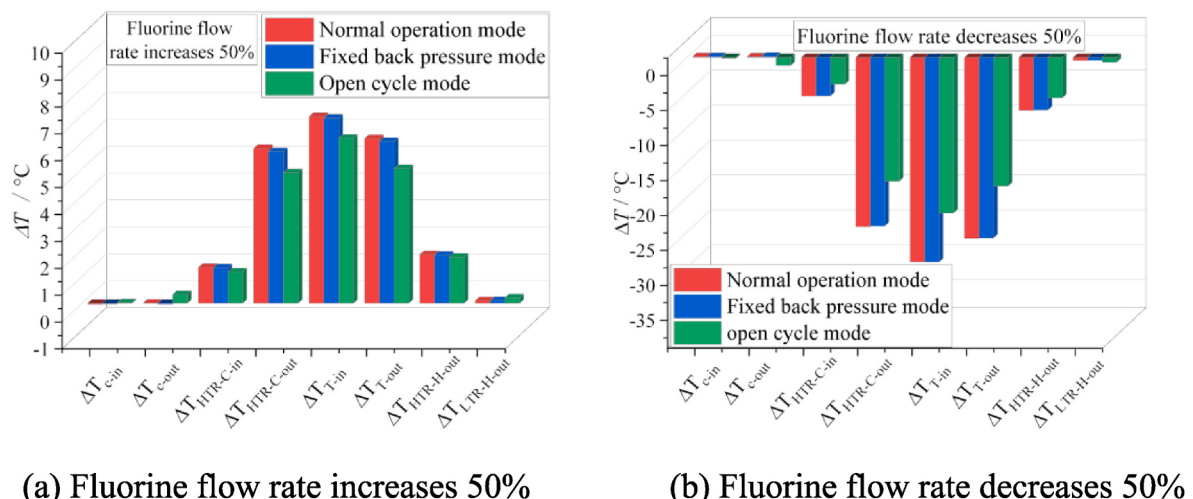


Fig. 22. Temperature change amplitudes for key parameters under fluorine flow rate disturbance with different operation mode.

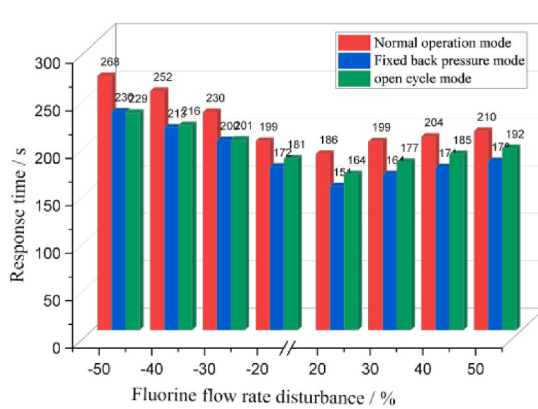
(a) Response time of SCO₂ cycle

Fig. 23. Response time and efficiency of SCO₂ cycle under fluorine flow rate disturbance with different operation mode.

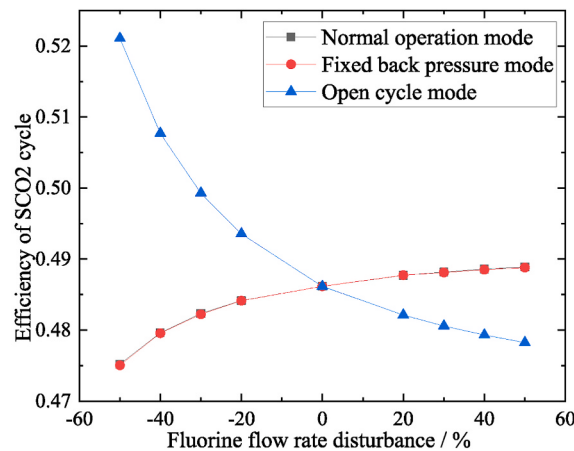
operation mode is about 185s–267.5 s, and it is longer than others since the joint influence of iteration temperature and pressure. Furthermore, the response time under heat fluorine flow rate decreasing conditions is longer than that under heat fluorine flow rate increasing conditions. It can be owed to the large temperature change amplitude under heat fluorine flow rate decreasing conditions.

The efficiency of SCO₂ cycle is shown in Fig. 23(b). The efficiency of SCO₂ cycle with fixed pressure mode and normal operation mode are similar, and they increase with rise of heat fluorine flow rate gradually. According to the figures shown in Figs. 20 and 21, the temperature and pressure at turbine inlet are similar for these two modes, and the operation parameter disturbance at compressor inlet become very small, then the cycle efficiencies are similar to each other. The tendency of SCO₂ cycle efficiency with open cycle mode decreases with rise of heat fluorine flow rate, which is inverse to others. It is because that with open cycle mode, the compressor consumption power increases a lot, but turbine power increases slightly when heat fluorine flow rate increases. It is worth to note that, in this SCO₂ cycle, the designed temperature difference between heat fluorine and SCO₂ at heater is very large, thus the change of fluorine flow rate has little effect on efficiency of SCO₂ cycle. As the design temperature difference small, or the temperature difference is fixed, the efficiency of SCO₂ cycle may change a lot and dynamic character will be different, which will be discussed in future research.

4. Conclusion

A dynamic simulation model of the SCO₂ cycle was established with Matlab Simulink software. The dynamic characters of SCO₂ cycle and the related facilities were investigated with different turbine back pressure modes, such as normal operation mode (unconfined back pressure), fixed pressure mode and open loop mode. The main conclusions can be summarized as follows.

- 1) HTR and LTR are larger in volume and thermal power than others. For the dynamic characteristics of the heat exchangers under different perturbations, the response time of the recuperator is about 4–5 times of the response time of the precooler and heater. For the dynamic characteristics of the SCO₂ cycle, the temperature response of the HTR and LTR is slower and the temperature variations of the HTR and LTR are larger, resulting in a long response time of the SCO₂ cycle.
- 2) Under the cold end parameter perturbation, the response characteristics under normal operation mode and fixed backpressure mode

(b) Efficiency of SCO₂ cycle

show similar response characteristics since effect of temperature and SCO₂ flow rate iteration. Under the heat source parameter perturbation, the iterative effect of temperature can be neglected, and system response times in the fixed pressure mode and open loop mode are approximately equal.

- 3) The differences in the dynamic characteristics of the SCO₂ cycle in different turbine back pressure modes indicate that the effect of pressure iteration on the SCO₂ system characteristics is less important than that of temperature iteration. It proved the system parameters in the fixed pressure mode are relatively stable, and the parameters variations are small under different perturbations.

CRediT authorship contribution statement

Quanbin Zhao: Writing – original draft, Methodology, Funding acquisition, Data curation. **Jiayuan Xu:** Writing – review & editing, Investigation, Data curation. **Min Hou:** Investigation, Formal analysis, Data curation, Dalin Zhang, Supervision, Resources, Project administration, Funding acquisition, Conceptualization. **Daotong Chong:** Writing – review & editing, Validation, Supervision, Project administration, Funding acquisition, Conceptualization. **Jinshi Wang:** Writing – review & editing, Supervision, Formal analysis. **Weixiong Chen:** Formal analysis, Data curation, Conceptualization.

Declaration of competing interest

We declare that we have no financial and personal relationships with other people or organizations that can inappropriately influence our work; there is no professional or other personal interest of any nature or kind in any product, service and/or company that could be construed as influencing the position presented in, or the review of, the manuscript entitled.

Data availability

Data will be made available on request.

Acknowledgements

This work was supported by the National Key R&D Program of China (No.2020YFB1902003), and Young Talent fund of University Association for Science and Technology in Shaanxi, China (No. 20210406).

References

- [1] Brun Klaus, Friedman Peter, Dennis Richard. Fundamentals and applications of supercritical carbon dioxide (sCO₂) based power cycles[M]. Woodhead Publisher; 2017.
- [2] Li G, Du G, Liu G, Yan J. Study on the dynamic characteristics, control strategies and load variation rates of the concentrated solar power plant. *Appl Energy* 2024; 357.
- [3] Sun E, Wang X, Qian Q, Li H, Ma W, Zhang L, Xu J. Proposal and application of supercritical steam Rankine cycle using supercritical reheating regeneration process and its comparison between S-CO₂ Brayton cycle. *Energy Convers Manag* 2023;280.
- [4] AlSulaiman FA, Atif M. Performance comparison of different supercritical carbon dioxide brayton cycles integrated with a solar power tower[J]. *Energy* 2015;82: 61–71.
- [5] Sarkar J. Second law analysis of supercritical co₂ recompression brayton cycle[J]. *Energy* 2009;34(9):1172–8.
- [6] Akbari AD, Mahmoudi SM. Thermo-economic analysis & optimization of the combined supercritical co₂ (carbon dioxide) recompression brayton/organic rankine cycle[J]. *Energy* 2014;78:501–12.
- [7] Fourspring PM, et al. Testing of compact recuperators for a supercritical CO₂ Brayton power cycle. In: 4th international symposium on supercritical CO₂ power cycles. Pittsburgh, PA, USA; 2014.
- [8] Sienicki JJ, Moisseytsev A, Fuller RL, et al. Scale dependencies of supercritical carbon dioxide brayton cycle technologies and the optimal size for a nextstep supercritical co₂ cycle demonstration[C]. SC02 power cycle symposium; 2011.
- [9] Weiland N, Thimsen D. A practical look at assumptions and constraints for steady state modeling of sCO₂ Brayton power cycles [R]. 2016.
- [10] Moisseytsev A, Sienicki JJ. Development of a plant dynamics computer code for analysis of a supercritical carbon dioxide brayton cycle energy converter coupled to a natural circulation lead-cooled fast reactor[R]. Argonne National Laboratory; 2006.
- [11] Moisseytsev A, Sienicki JJ. Transient accident analysis of a supercritical carbon dioxide Brayton cycle energy converter coupled to an autonomous lead-cooled fast reactor. *Nucl Eng Des* 2008;238(8):2094–105.
- [12] Moisseytsev A, Sienicki JJ. Development of the ANL plant dynamics code and control strategies for the supercritical carbon dioxide brayton cycle and code validation with data from the sandia small-scale supercritical carbon dioxide brayton cycle test loop[R]. Argonne National Laboratory; 2011.
- [13] Moisseytsev A, Sienicki J. Dynamic control analysis of the AFR-100 SMR SFR with a supercritical CO₂ cycle and dry air cooling: Part I — plant control optimization [C]. London, UK: Proceedings of the 26th International Conference on Nuclear Engineering; 2018.
- [14] Carstens NA. Control strategies for supercritical carbon dioxide power conversion systems[D]. Massachusetts Institute of Technology; 2007.
- [15] Gao C, Wu P, Liu W, et al. Development of a bypass control strategy for supercritical CO₂ Brayton cycle cooled reactor system under load-following operation[J]. *Ann Nucl Energy* 2021;151:107917.
- [16] Wu P, Ma Y, Gao C, et al. A review of research and development of supercritical carbon dioxide Brayton cycle technology in nuclear engineering applications[J]. *Nucl Eng Des* 2020;368:110767.
- [17] Dostal V. A supercritical carbon dioxide cycle for next generation nuclear reactors [D]. Massachusetts Institute of Technology; 2004.
- [18] Oh BS, Ahn YH, Kim SG, et al. Transient analyses of S-CO₂ cooled kaist micro modular reactor with gamma+ code[C]. San Antonio, USA: The 5th International Symposium - Supercritical CO₂ Power Cycles; 2016.
- [19] Wang R, Wang X, Shu G, Tian H, Cai J, Bian X, Li X, Qin Z, Shi L. Comparison of different load-following control strategies of a sCO₂ Brayton cycle under full load range. *Energy* 2022;246.
- [20] Berthet Couso G, Barraza Vicencio R, Vasquez Padilla R, et al. Dynamic model of supercritical co₂ brayton cycles driven by concentrated solar power[C]//the ASME 2017 Nuclear Forum. American Society of Mechanical Engineers Digital Collection; 2017.
- [21] Bian X, Wang X, Wang R, Cai J, Tian H, Shu G, Lin Z, Yu X, Shi L. A comprehensive evaluation of the effect of different control valves on the dynamic performance of a recompression supercritical CO₂ Brayton cycle. *Energy* 2022;248.
- [22] Sun E, Xu J, Li M, Liu G, Zhu B. Connected-top-bottom-cycle to cascade utilize flue gas heat for supercritical carbon dioxide coal fired power plant. *Energy Convers Manag* 2018;172:138–54.
- [23] Li G, Liu G, Du G, Wang J, Yan J. UTOP accident analysis and mitigation measures of lead-cooled fast reactor considering coupling effect with SC02 Brayton cycle. *Prog Nucl Energy* 2023;166.
- [24] Vamsi K, Avadhanula Timothy J. Held. Integrated transient modeling of gas turbine and sCO₂ power cycle for exhaust heat recovery application[C].The 7th international supercritical CO₂ power cycles symposium. 2022. San Antonio, Texas.
- [25] Park JH, Bae SW, Park HS, Cha JE, Kim MH. Transient analysis and validation with experimental data of supercritical CO₂ integral experiment loop by using MARS. *Energy* 2018;147:1030–43.
- [26] Wang X, Cai J, Lin Z, Tian H, Shu G, Wang R, Bian X, Shi L. Dynamic simulation study of the start-up and shutdown processes for a recompression CO₂ Brayton cycle. *Energy* 2022;259. <https://doi.org/10.1016/j.energy.2022.124928>.
- [27] Singh R, Miller SA, Rowlands AS, et al. Dynamic characteristics of a direct-heated supercritical carbon-dioxide Brayton cycle in a solar thermal power plant[J]. *Energy* 2013;50:194–204.
- [28] Olumayegun O, Wang M. Dynamic modelling and control of supercritical CO₂ power cycle using waste heat from industrial processes [J]. *Fuel* 2019;249:89–102.
- [29] Hu H, Guo C, Cai H, Jiang Y, Liang S, Guo Y. Dynamic characteristics of the recuperator thermal performance in a S-CO₂ Brayton cycle. *Energy* 2021;214: 119017.
- [30] Deng T, Li X, Wang Q, Ma T. Dynamic modelling and transient characteristics of supercritical CO₂ recompression Brayton cycle. *Energy* 2019;180:292–302.
- [31] Ingersoll D, Forsberg C, Ott L, et al. Status of preconceptual design of the advanced high-temperature reactor (AHTR)[R]. Oak Ridge National Laboratory; 2004.
- [32] Greene S, Gehin J, Holcomb D, et al. Pre-conceptual design of a fluoride-salt-cooled small modular advanced high temperature reactor (SmAHTR)[R]. Oak Ridge National Laboratory; 2011.
- [33] Dyreby JJ. Modeling the supercritical carbon dioxide Brayton cycle with recompression[D]. University of Wisconsin-Madison; 2014.
- [34] Lee J, Lee J, Ahn Y, et al. Design methodology of supercritical CO₂ brayton cycle turbo-machineries[C]. In: ASME turbo expo 2012: turbine technical conference and exposition, gyeongju, korea; 2012.
- [35] Ma YG, Morozuk Tatiana, Liu M, Liu JP. Development and comparison of control schemes for the offdesign operation of a recompression supercritical CO₂ cycle with an intercooled main compressor. *Energy* 2020;119011.
- [36] Ma T, Li M, Xu J, et al. Thermodynamic analysis and performance prediction on dynamic response characteristic of PCHE in 1000 MW S-CO₂ coal fired power plant [J]. *Energy* 2019;175:123–38.